Synchronization of stochastic oscillations due to long-range diffusion

A. Efimov,[1] A. Shabunin,[1] and A. Provata[2]
[1]*Department of Physics, Saratov State University, Astrakhanskaya 83, Saratov 410026, Russia*
[2]*Institute of Physical Chemistry, National Center for Scientific Research "Demokritos," 15310 Athens, Greece*
(Received 28 February 2008; revised manuscript received 9 June 2008; published 5 November 2008)

We investigate the effect of long-range diffusive mixing on stochastic processes taking place on low-dimensional catalytic supports. As a working example, the cyclic lattice Lotka-Volterra (LLV) model is used which is conservative at the mean-field level and demonstrates fractal patterns and local oscillations when realized on low-dimensional lattice supports. We show that the local oscillations are synchronized when a weak, long-range, diffusive process is added to LLV and global oscillations of limit cycle type emerge. This phenomenon is demonstrated as a nonequilibrium phase transition and takes place when the mixing-to-reaction rate p (order parameter) is above a critical point p_c. The value of the critical point is shown to depend on the kinetic parameters. The global oscillations in this case emerge as a result of phase synchronization between local oscillations on sublattices.

DOI: 10.1103/PhysRevE.78.056201 PACS number(s): 05.45.−a, 05.40.−a, 64.60.Ht, 87.23.Cc

I. INTRODUCTION

Synchronization of interacting systems is a key phenomenon of nature and is often discovered in the background of self-organization processes in physics, chemistry, biology, and other sciences [1]. Having been discovered first in ensembles of periodic self-sustained oscillators, it was spread later to chaotic systems [2]. There are two basic definitions for synchronization in complex oscillations:

(i) Generalized synchronization, a deterministic interconnection between the time series of two coupled subsystems A and B, $x_A(t)=G[x_B(t)]$ [3].

(ii) Phase synchronization, the phenomenon of instantaneous phases locking [4] which is also characterized by frequency adjustment [5] and coherence increase [6] in oscillators spectra.

Phase synchronization can be formally defined as locking between instanteneous phases $\Phi_{A,B}$ of the time series in the subsystems A and B: $\lim_{t\to\infty}|\Phi_A(t)-\Phi_B(t)|<M$, where M is a positive value. This relation signals the presence of correlation between phases, while instantaneous amplitudes remain uncorrelated. In particular, phase synchronization is a classical property for self-sustained oscillators and may take place in the presence of noise [7] and even in dynamical systems driven by external noise [8].

While most early works concentrated on synchronization in deterministic networks of oscillators, recent attention has been devoted to synchronization of stochastic interactions between units with several discrete states which can demonstrate oscillation behavior as cooperative phenomenon [9–12]. In Ref. [10] the authors demonstrate that when the probability of transitions between states (which plays the role of coupling) crosses a critical point, global synchronization occurs on the lattice. In Refs. [11,12] the authors study the synchronization in two reactive processes, the rock-scissors-paper (RSP) game and the susceptible-infected-refractory (SIR) system, respectively. Both cases are treated as small world networks, where the permanent or temporal network connectivity (internal disorder) provides the coupling between the different units. Synchronization in the RSP and SIR cases arises when the disorder rate in the networks exceeds a certain critical threshold.

In this study we provide a different example of an external coupling mechanism on a lattice model, which can also lead to global synchronization. This mechanism is a long-range diffusion between elements of the lattice. The parameter of the diffusion can be interpreted as a strength of coupling between subparts of the lattice. In our case coupling increase also leads to oscillating behavior of the system, which is demonstrated as the analog of a Hopf bifurcation in ordinary differential equations. In contrast to [11,12], the diffusive mechanism proposed here is a result of an external random force and not an internal disorder of the network. More detailed analysis showed that the observed oscillations are a result of a phase synchronization process taking place between oscillations on separate parts of the lattice. Thus, the pure stochastic model with discrete phase space on the large scale demonstrates typical oscillatory phenomena: Limit-cycle behavior and phase synchronization.

As a model we consider a lattice compatible system, evident in chemical reactions and population dynamics, where periodicity is attributed to the process dynamics while local coupling is provided by the support (e.g., in heterogeneous catalytic reactions, diffusion, and population dynamics) [13,14]. A short description of the system, its mean-field (MF) model, and results of Monte Carlo (MC) simulations are presented in Sec. II. In Sec. III we investigate the properties of the system under long-range diffusion both on microlevel and macrolevel. Section IV describes process of phase synchronization between local oscillations on the lattice. In the concluding section the main results are summarized and open problems are presented.

II. LLV MODEL

The choice of the system under study was motivated by problems in population dynamics and reactive dynamics taking place on low-dimensional or catalytic supports. The search for a simple, lattice compatible model, with center type of mean-field behavior led us to the choice of the lattice

Lotka-Volterra (LLV) system for this study [15,16]. As a support for the LLV model a square regular lattice containing $N=L\times L$ sites is considered, with every site being in one of three possible states (occupying species): X, Y or S. For each site the transitions from one state to another are governed by the interactions with the neighbors according to the following scheme:

$$X + Y \xrightarrow{k_1} 2Y, \tag{1a}$$

$$Y + S \xrightarrow{k_2} 2S, \tag{1b}$$

$$S + X \xrightarrow{k_3} 2X, \tag{1c}$$

where $k_i, i=1,2,3$ are the kinetic parameters. The basic rule for the realization of schemes (1a)–(1c) is that a randomly chosen site at state X transforms to state Y with probability proportional to k_1 provided that a randomly chosen neighbor is in state Y. The same rules hold cyclically for the other states.

If the lattice represents an autocatalytic support, X and Y can be interpreted as chemical species, which occupy the lattice sites, while S may represent a vacant site. According to this interpretation, step (1a) is autocatalytic reaction, while steps (1b) and (1c) denote desorption and adsorption of Y and X particles, respectively. Alternatively, the reactive scheme may represent a population dynamic model where step (1a) represents nonlinear interaction between species X and Y, while steps (1b) and (1c) represent death of Y species and birth of X species, respectively.

From the dynamical point of view the LLV model can be described by the MF rate equations [16],

$$\dot{x} = -k_1 xy + k_3 x(1-x-y), \tag{2a}$$

$$\dot{y} = k_1 xy - k_2 y(1-x-y), \tag{2b}$$

where x and y are the relative concentrations. The phase space of system (2a) and (2b) has four equilibrium points: Three saddle points $P_1(0;0)$, $P_2(1;0)$, $P_3(0;1)$, and a center $P_4(k_2/K;k_3/K)$ $(K=k_1+k_2+k_3)$. The saddles and their invariant manifolds, M_1, $x=0$; M_2, $y=0$; M_3, $x+y=1$ form a closed triangular contour. This contour bounds the region in the phase space where chemical or biological interpretation makes sense. Inside the contour, oscillations remain finite; outside the contour, all trajectories go to infinity. If the initial conditions are chosen within the range $0\leqslant x, y, s\leqslant 1$, the model demonstrates conservative periodic oscillations and the phase portrait of the system consists of an infinite number of closed trajectories around the center P_4 [16].

The MF approach does not take into account the local nature of the processes on the lattice and therefore can only serve as a very rough model for dynamical processes on a support. An alternative tool for modeling the LLV scheme is the kinetic Monte Carlo (KMC) simulation in which the transition of a lattice site from one state to another at a particular time step depends on the precise state of the first neighbors on the lattice. The microscopic simulation rules are given in detail in Ref. [16] but a brief recapitulation of them is as follows:

(i) At every elementary time step (ETS) one lattice site and one of its neighboring sites are randomly selected.

(ii) If the selected site is in state X and the neighbor in state Y the selected particle transforms to Y with probability $p_1=k_1/\max\{k_1,k_2,k_3\}$, otherwise it remains in the original state.

(iii) Similar rules hold for the states Y and S, cyclically, with respective probabilities $p_{2,3}$.

In the KMC process $N=L\times L$ ETS constitute 1 Monte Carlo step (MCS). During 1 MCS all lattice sites have on the average one chance to react. As the simulation process progresses the spatial distributions of X and Y particles change from one MCS to another, providing the evolution of the system at the microscopic level. To make a bridge between the microlevel and the macrolevel it is reasonable to use the x and y variables which represent the average partial concentrations,

$$x = N_X/N, \quad y = N_Y/N, \tag{3}$$

where $N_{X(Y)}$ is the number of $X(Y)$ particles.

KMC simulations demonstrate that the time evolution of x and y contains two stages: (a) A short oscillatory, transient process followed by (b) stochastic oscillations around some steady state value. This last value is very well predicted from the MF approach, being equal to the fixed point P_4. In Fig. 1(a) the evolution of initial values $x_0=x(0)$ and $y_0=y(0)$ far from the point P_4 are depicted. A transient process is observed after which the values tend to the neighborhood of the equilibrium point P_4. The intensity of the steady state oscillations sensibly depends on the lattice size. This can be seen in Fig. 1(b) where the time series of the x concentration on the 512×512 sites lattice (solid line) and on its 128×128 sites sublattice (dashed line) are depicted. A more detailed analysis of the intensity (the square root of the dispersion, σ_x) dependence on the lattice size evidences that it is reduced as

$$\sigma_x \sim 1/\sqrt{N}. \tag{4}$$

The correspondent plot is depicted in Fig. 2 in the log-log scale. Oscillations tend to zero when the lattice size tends to infinity. Consequently, in the KMC process P_4 behaves as a dissipative, stable focus point which attracts all trajectories started throughout its basin. This disagreement between results of MF and KMC approaches has been noted in a number of works (see, for example, [16,17]) while the detailed analysis of them is presented in [18]. However, in any finite window at any stage of the above KMC processes, the concentration oscillations are preserved locally on the system (local oscillators) [16].

It is noted here, that the MF regime can be achieved in the KMC simulations via long-range reactive coupling between randomly selected distant units. In the KMC simulations, this means that the chosen particles do not interact with their immediate neighbors but equiprobably with any randomly selected particle within a distance l_r (l_r is defined as the minimum number of steps which is necessery to achieve two

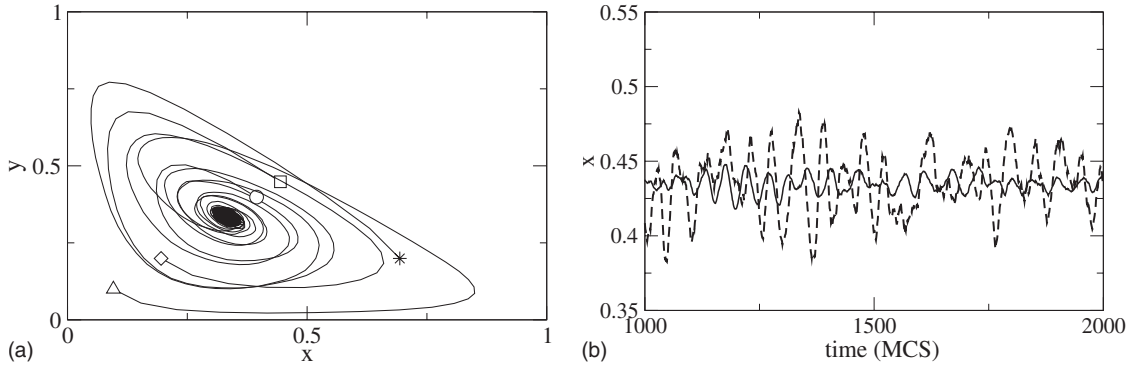

FIG. 1. (a) Phase portraits on the x-y plane for different initial values: (○) $x=0.4$, $y=0.4$; (□) $x=0.45$, $y=0.45$; (◇) $x=0.2$, $y=0.2$; (△) $x=0.1$, $y=0.1$; (∗) $x=0.1$, $y=0.7$. (b) Time series of the x concentration on the whole lattice (solid line) and on a subpart of 128×128 elements (dashed line). Parameter values are $k_1=0.6$, $k_2=0.8$, $k_3=1$.

distant points on the lattice). In Fig. 3 the KMC results of the LLV are shown for parameters values $k_1=k_2=k_3=1.0$, lattice size $L=512$, and reactivity range $l_r=300$. Starting from three different initial conditions (as indicated on the graph) the system performs oscillations whose amplitude depends on the initial conditions. This is clearly center-type behavior as in the case of the mean field. This is not an unexpected result since the most significant condition for the validity of the mean-field description is that every particle interacts equally with all other particles in the system. This clearly holds in the case of the long-range reactive coupling and thus the MF regime is approached.

Let us try a different coupling process on the lattice to synchronize its behavior. It is obvious that synchronization cannot be achieved by increasing the probabilities p_i: Simultaneous change of all p_i does not lead to any qualitative changes in the behavior but only in a change of the time scale of the processes. Alternatively, by changing only one of the p_i, $i=1,\ldots,3$ can result in fast poisoning of the finite lattice by some component (X or Y). A possible way for physically motivated coupling is to add a short-range (local) or a long-range (global) diffusive coupling on it. The last case is the subject of the next section.

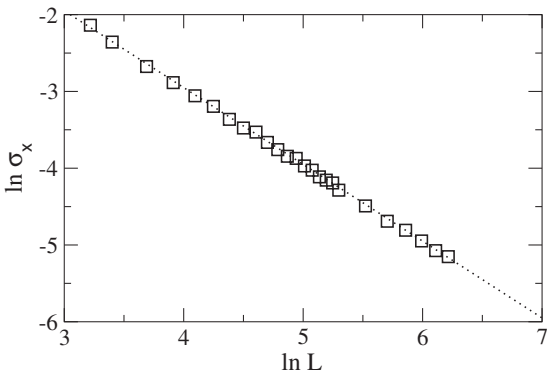

FIG. 2. Dependence of the intensity of x—oscillations on the lattice size L in the log-log scale. Parameters values are $k_1=0.6$, $k_2=0.8$, $k_3=1$.

III. GLOBAL OSCILLATION IN THE LLV SYSTEM WITH EXTERNAL LONG-RANGE DIFFUSION

In an attempt to synchronize the local oscillators on the lattice, global diffusive coupling is introduced, in the form of exchange of state between randomly chosen lattice sites. This additional process, independent of the original scheme (1a)–(1c), may be a result of an external shuffling allowing for immediate states exchange between distant lattice units. In the case of autocatalytic surface reactions, some transport agent that is not involved in the reactions may be responsible for the mixing. In the case of population dynamics such a mixing may be realized by the natural migration processes.

To define more precisely this long-range diffusion mechanism, it is necessary to define first the relative frequency of diffusive-to-reactive events, p,

$$p=(n/N), \tag{5}$$

where n is the number of diffusive steps in 1 MCS, while N is the total number of reactive attempts in 1 MCS. The diffusion range l_d is also defined. This means that particles can diffuse randomly to any site within the range $[1,l_d]$, note that $1\leqslant l_d\leqslant 2L$ ($2L$ is the maximum distance on the $L\times L$ lattice). In our research we used the maximum possible value of

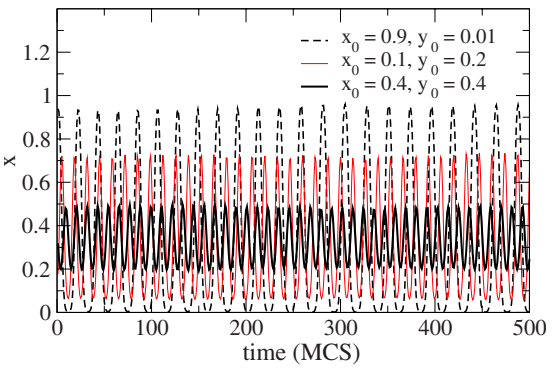

FIG. 3. (Color online) Long-range reactive coupling in the LLV model. The lattice size is $L=512$, the reactivity range is $l_r=300$ and the parameters are $k_1=k_2=k_3=1.0$. Initial conditions are indicated on the graph.

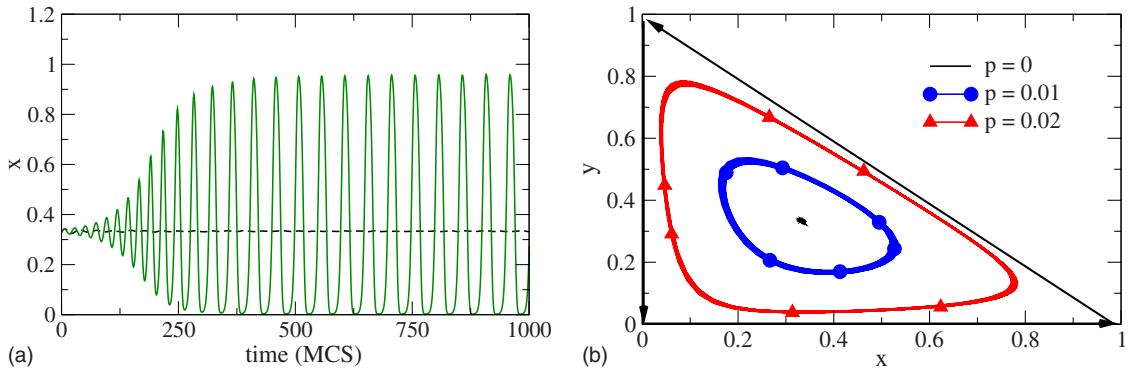

FIG. 4. (Color online) (a) The time series of $x(t)$ for the lattice without diffusion (green curve) and with weak diffusion, $p=0.03$ (black dashed curve). (b) Attractors for different values of p. Straight lines depict the triangle of the invariant manifolds in (2a) and (2b). Parameters of the system are $k_1=k_2=k_3=1$, $L=1024$.

l_d, $l_d=2L$. Additional properties of the long-range diffusion process considered here are as follows:

(i) For every exchange event two lattice sites are randomly and independently chosen and their states are exchanged.

(ii) The distance between the exchanged particles must be less or equal to the diffusion range l_d.

(iii) The exchange is independent of the sites' positions.

If the probability $p \to 1$, then total mixing is attained, while for $p \to 0$ the mixing is weak and the behavior described above and in Ref. [16] is observed.

Although the long-range diffusive coupling does not change directly the average concentrations x and y, as this study demonstrates, it causes dramatic changes in the system dynamics both at the microlevel and macrolevel. Considering the global behavior, the time series $x(t)$ for $p=0$ (green line) and $p=0.03$ (black line) are depicted in Fig. 4(a). It is clear that global, almost periodic oscillations with sufficiently large amplitude are observed, even for relatively low values of p. This amplitude no longer depends on the size of the lattice but characterizes the oscillation itself.

The shape of the oscillations in Fig. 4(a) resembles the one expected from the MF prediction. However, while the MF oscillation is conservative, this KMC oscillation is of different nature. After an initial, transitory stage (for times $\sim$0–300 MCS) the system reaches a stable, almost periodic attractor (steady state). In Fig. 4(b) such phase portraits are shown for $p=0.01$ (curve marked by ○) and $p=0.02$ (curve marked by △).

For finite lattice sizes the shape of these attractors looks like a noisy limit cycle or like a weak chaotic attractor in an ordinary differential equation (ODE) system. When the lattice size tends to ∞, the stochastic fluctuations vanish and the dynamics tend to a periodic, limit cycle, global oscillation.

Next the dependence of the global oscillations on the parameter p are examined. In Fig. 5 the square of the amplitude (dispersion, σ^2) of the oscillations as a function of p is plotted, for different values of k_1. When the rate p is sufficiently small, there are no observable changes of the system dynamics and the system behaves as the ordinary LLV model [16]. Global oscillations are not observed and there is only a small noise background which becomes smaller with increasing lattice size. Then, at the critical point p_c the focus loses its stability and global oscillations appear in its neighborhood. Increasing further the diffusion-reaction rate $p > p_c$ results in monotonous linear growth of the dispersion. In this regime the oscillation amplitude increases as the square root of the difference between the instantaneous value of p and its critical value,

$$\sigma(p) \sim \sqrt{p - p_c}. \tag{6}$$

The global oscillations in the lattice KMC simulations spring exactly as a limit cycle after the supercritical Hopf bifurcation in the theory of dynamical systems. Increasing p further increases the cycle thus shifting it from the central point P_4 in the direction of the triangle contour of the invariant manifold defined by the saddle points P_1, P_2, P_3. During this process the shape of the oscillation changes, becoming more relaxationlike [see curve (△) in Fig. 4]. If the mixing is strong enough the trajectories approach closely the contour and at the particular value of the mixing rate they collide with it, leading to poisoning of the lattice by one of the three components. Figure 5 depicts three curves of $\sigma^2(p)$ for different values of parameter k_1. The critical point p_c is seen to depend on the parameters k_i of the system. More detailed analysis demonstrates that p_c depends on the imbalance degree of the parameters k_i. The greater the difference of parameters, the smaller the critical value of p. In this case the poisoning of the lattice occurs at lower p values. Additional analysis of the global oscillations has shown that the ampli-

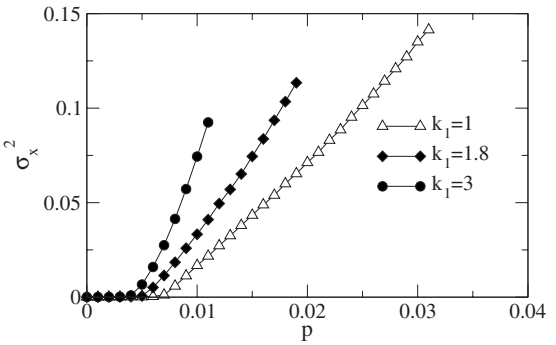

FIG. 5. Dispersion of $x(t)$ versus the diffusion-reaction rate p for different values of k_1. Other parameters are fixed in $k_2=k_3=1$.

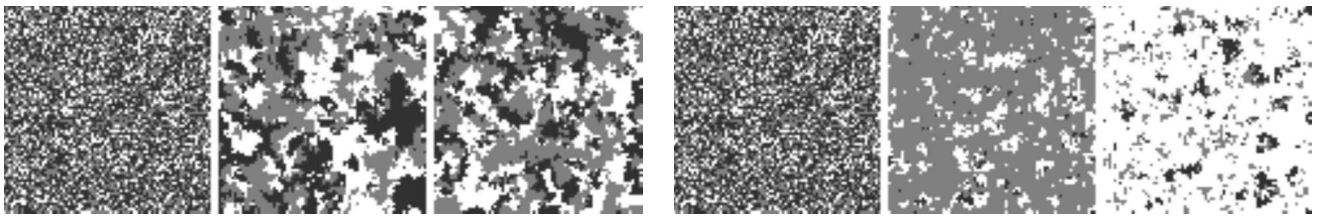

FIG. 6. Lattice snapshots at successive time intervals (from the left-hand to the right-hand sides): 0 MCS, 1000 MCS, 1500 MCS for (a) $p=0.00$ and (b) $p=0.016$. Parameters values are $k_1=0.6$, $k_2=0.8$, $k_3=1$.

tude σ and the critical value of p do not depend on the lattice size if the last is sufficiently large, while for small lattices, $L \leqslant 300$, there is lattice size dependence.

The essential change of the global behavior evidently must be a consequence of changes at the microlevel. In the case of $p=0$ (see Fig. 6 and [16]) from an initial random distribution spontaneous clustering takes place and cluster-cluster competition, where the clusters interact with one another through their boundaries, while their interiors remain intact. Even in the case of small rate $p<p_c$, the cluster borders seem to be the main interaction regions, with a number of small encapsulations that appear inside the clusters due to weak mixing. These encapsulations do not contribute significantly in the dynamics for large system sizes. Thus for $p \leqslant p_c$ local regions on the lattice oscillate out-of-phase and this results in suppression of the global oscillations.

After crossing p_c the behavior of the lattice essentially changes. In Fig. 6 almost the entire lattice is shown to be periodically colored by one type of species indicating that the lattice now behaves synchronously.

IV. PHASE SYNCHRONIZATION BETWEEN OSCILLATIONS ON SUBLATTICES

It is evident, that global oscillations on the lattice must be a consequence of synchronization between oscillations of its subparts. To understand this process the average concentrations of X species on two sublattices (denoted as A and B), $x_A(t)$ and $x_B(t)$, are calculated as a function of time. The lattice size is $L=1024$ while the sublattices have linear sizes $l=64$. The corresponding time series is plotted in Fig. 7. When the mixing is absent, the oscillations x_A and x_B look asynchronous [Fig. 7(a)]. Additional mixing leads to increasing their amplitudes and to phase synchronization in the regime of global oscillations. This can be seen in Fig. 7(b) as an overlap of the maximums of both time series. The fact of phase synchronization can be demonstrated more clearly if we compute the time dependence of their phase difference. In Fig. 8 the phase difference $\Delta\Phi=\Phi_A-\Phi_B$ between sublattices A and B is plotted, defined as

$$\Phi_{A(B)} = \mathrm{arctg}\left(\frac{y_{A(B)} - \langle y_{A(B)}\rangle}{x_{A(B)} - \langle x_{A(B)}\rangle}\right). \tag{7}$$

For $p(=0)<p_c \simeq 0.007$ the local oscillators demonstrate random phases, and the phase difference curve has the form of Brownian motion, indicating uncorrelated phases. In the regime of global oscillations, for $p>p_c$, the phase difference is bounded near zero, so the phases of the local oscillators are locked demonstrating the classical phase synchronization phenomenon. The intermediate case is shown in the figure for $p=0.007$, which is very close to the threshold value. Here we see the imperfect phase synchronization, when time intervals of phase locking are randomly interrupted by intervals where the phase difference slips.

The phase synchronization of oscillations can be demonstrated also if we introduce a parameter mismatch between the two sublattices. For this purpose we will consider one of the kinetic parameters, k_1, as a random, sublattice dependent value,

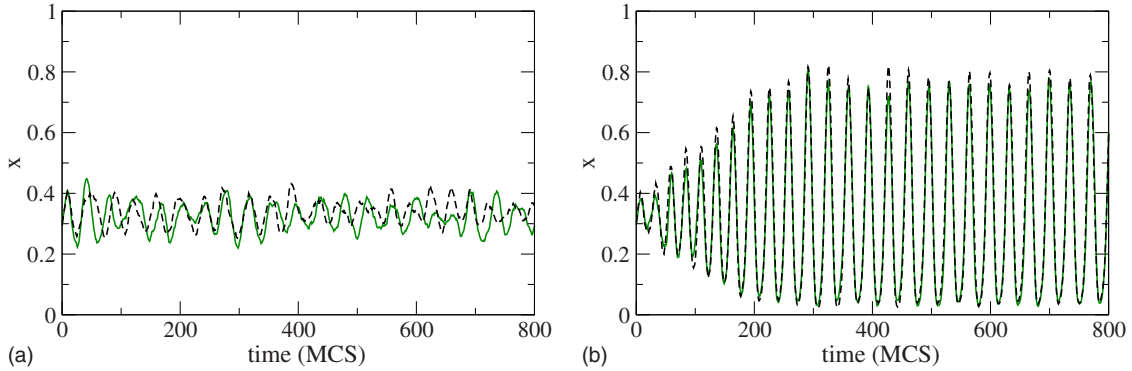

FIG. 7. (Color online) Time series of oscillations on two different sublattices: $x_A(t)$ (solid green line) and $x_B(t)$ (dashed black line) for (a) $p=0$ and (b) $p=0.02$. Parameter values are $k_1=1.0$, $k_2=1.0$, and $k_3=1.0$.

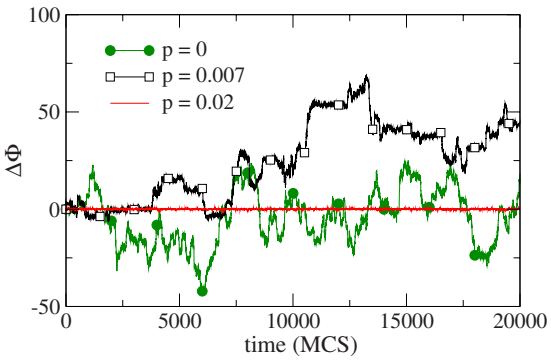

FIG. 8. (Color online) Phase differences for two local oscillators as a function of time at different mixing rates. Parameter values are $k_1=k_2=k_3=1$.

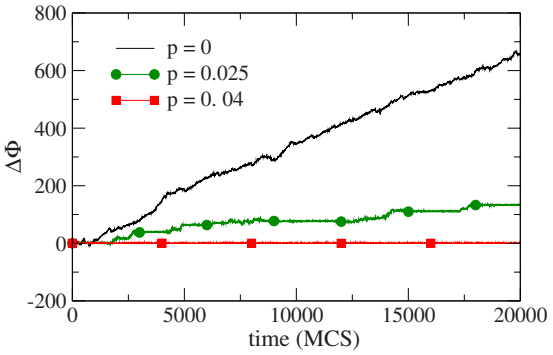

FIG. 9. (Color online) Evolution of the phase difference between two local oscillators on the lattice with mismatch of parameter k_1, $k_1^A=0.376$ and $k_1^B=0.703$. Other parameters are $k_2=k_3=1$.

$$k_1^{(i,j)} = f(i,j), \tag{8}$$

where f is a random function with values homogeneously distributed in the range $[0; 1]$, $i,j=1,2,\ldots$ are discrete variables denoting the sublattice indices. In our case the $N=1024\times1024$ sites lattice has been divided to 16×16 sublattices, which are characterized by their own value of $k_1^{(i,j)}(i,j=1,2,\ldots,16)$. As in the preceding paragraph we followed oscillations on the chosen sublattices (A) and (B), which, in our case, had the following parameter values: $k_1^A=0.376$ and $k_1^B=0.703$. Since the value of k_1 influences the basic frequency of oscillations, in the system without mixing (or with $p<p_c$) all sublattices are characterized by their own frequency. Therefore, the difference between the phases of the partial oscillators increases with time (see curve 1 in Fig. 9) and this reflects that the average periods of the oscillations are no longer equal. This case is related to the absence of phase synchronization between local oscillations. Increasing of the mixing parameter p towards the critical point results in imperfect phase synchronization. It means that in the temporal behavior of the phase difference we can observe intervals of synchronous behavior when the phases remain locked, which are interrupted by intervals when the instantaneous phases slip (see curve 2 in Fig. 9). Then, at sufficiently large p, phases remain locked at any moment of time (curve 3 in Fig. 9). This is the stage of perfect phase synchronization.

V. CONCLUSIONS

In conclusion, the influence of an external, random, long-range diffusive force on distributed, interacting particle systems was studied, using as working example the lattice Lotka-Volterra (LLV) model on the square lattice.

As was previously shown, while the LLV model demonstrates MF conservative (noise-sensitive) oscillations, when it is is realized on a lattice support via KMC simulations the system is divided into local oscillators which oscillate out of phase that results in the suppression of global oscillations. The introduction of a long-range reactive coupling between different parts of the lattice leads to the expected MF, center-type behavior. In this study, it is shown that, when a weak random, long-range diffusive coupling is introduced the behavior changes drastically. The local oscillators are phase synchronized producing stable, global oscillations. It was demonstrated that this nonequilibrium, phase synchronization emerges as a Hopf-type bifurcation, above a critical diffusion-to-reaction rate p_c. This critical point is shown to depend on the kinetic parameters.

Preliminary results indicate that the present behavior is maintained in other conservative, center-type systems which are lattice compatible. That is, diffusion drives the noise sensitive system into a stable limit cycle via a Hopf-like bifurcation, when a system parameter crosses a critical point. Further studies are needed to investigate the influence of diffusive coupling in dynamical systems with different phase space characteristics, such as limit-cycle or chaotic mean-field behavior.

ACKNOWLEDGMENTS

The authors would like to thank N. Kouvaris and Professor G. Nicolis for helpful discussions.

[1] S. H. Strogatz, *Non-Linear Dynamics and Chaos* (Westview, New York, 1994); A. S. Pikovsky, M. G. Rosenblum, and J. Kurths, *Synchronization* (Cabridge University Press, Cambridge, England, 2001).
[2] H. Fujisaka and T. Yamada, Prog. Theor. Phys. **69**, 32 (1983); A. S. Pikovsky, Z. Phys. B: Condens. Matter **55**, 149 (1984).
[3] N. F. Rulkov, M. M. Sushchik, L. S. Tsimring, and H. D. I. Abarbanel, Phys. Rev. E **51**, 980 (1995).
[4] M. G. Rosenblum, A. S. Pikovsky, and J. Kurths, Phys. Rev. Lett. **76**, 1804 (1996).
[5] V. S. Anishchenko, T. E. Vadivasova, D. E. Postnov, and M. A. Safonova, Int. J. Bifurcation Chaos Appl. Sci. Eng. **2**, 633 (1992).
[6] A. Shabunin, V. Astakhov, and J. Kurths, Phys. Rev. E **72**, 016218 (2005).
[7] R. L. Stratonovich, *Selected Topics in the Theory of Random Noise* (Gordon and Breach, New York, 1963).
[8] B. Shulgin, A. Neiman, and V. Anishchenko, Phys. Rev. Lett.

75, 4157 (1995); A. Neiman, A. Silchenko, V. Anishchenko, and L. Schimansky-Geier, Phys. Rev. E **58**, 7118 (1998).
[9] H. Daido, Phys. Rev. Lett. **61**, 231 (1988).
[10] K. Wood, C. Van den Broeck, R. Kawai, and K. Lindenberg, Phys. Rev. Lett. **96**, 145701 (2006); Phys. Rev. E **75**, 041107 (2007).
[11] G. Szabo, A. Szolnoki, and R. Izsak, J. Phys. A **37**, 2599 (2004); A. Szolnoki and G. Szabo, Phys. Rev. E **70**, 037102 (2004); G. Szabo and G. Fath, Phys. Rep. **446**, 97 (2007).
[12] M. Kuperman and G. Abramson, Phys. Rev. Lett. **86**, 2909 (2001).
[13] G. Ertl, Science **254**, 1750 (1991); R. Imbihl and G. Ertl, Chem. Rev. (Washington, D.C.) **95**, 697 (1995); V. P. Zhdanov, Phys. Rev. E **60**, 7554 (1999); J. E. Satulovsky and T. Tome, J. Math. Biol. **35**, 344 (1997); R. Monetti, A. Rozenfeld, and E. Albano, Physica A **283**, 52 (2000).
[14] G. Nicolis and I. Prigogine, *Self-Organization in Non-Equilibrium Systems* (Wiley, New York, 1997); J. D. Murray, *Mathematical Biology* (Springer, Berlin, 1991).
[15] K. I. Tainaka, Phys. Rev. E **50**, 3401 (1994); L. Frachebourg, P. L. Krapivsky, and E. Ben-Naim, *ibid.* **54**, 6186 (1996); M. Schulz and S. Trimper, J. Phys. A **29**, 6543 (1996); L. Frachebourg and P. L. Krapivsky, *ibid.* **31**, L287 (1998).
[16] A. Provata, G. Nicolis, and F. Baras, J. Chem. Phys. **110**, 8361 (1999); A. V. Shabunin, A. Efimov, G. A. Tsekouras, and A. Provata, Physica A **347**, 117 (2005).
[17] G. A. Tsekouras and A. Provata, Phys. Rev. E **65**, 016204 (2001).
[18] M. Mobilia, I. T. Georgiev, and U. C. Tauberg, J. Stat. Phys. **128**, 447 (2006); T. Reichenbach, M. Mobilia, and E. Frey, Phys. Rev. E **74**, 051907 (2006).